

Real-Time Hand Gesture Recognition: Integrating Skeleton-Based Data Fusion and Multi-Stream CNN

Oluwaleke Yusuf, Maki Habib, Mohamed Moustafa

Abstract—This study focuses on Hand Gesture Recognition (HGR), which is vital for perceptual computing across various real-world contexts. The primary challenge in the HGR domain lies in dealing with the individual variations inherent in human hand morphology. To tackle this challenge, we introduce an innovative HGR framework that combines data-level fusion and an Ensemble Tuner Multi-stream CNN architecture. This approach effectively encodes spatiotemporal gesture information from the skeleton modality into RGB images, thereby minimizing noise while improving semantic gesture comprehension. Our framework operates in real-time, significantly reducing hardware requirements and computational complexity while maintaining competitive performance on benchmark datasets such as SHREC2017, DHG1428, FPHA, LMDHG and CNR. This improvement in HGR demonstrates robustness and paves the way for practical, real-time applications that leverage resource-limited devices for human-machine interaction and ambient intelligence.

Index Terms—Data-Level Fusion, Multi-Stream Convolutional Neural Network, Skeleton Modality, Ensemble Learning, Hand Gesture Recognition.

I. INTRODUCTION

Hand Gesture Recognition (HGR) plays a vital role in perceptual computing by enabling computers to capture and understand human hand gestures using mathematical algorithms. This technology enables computational devices to facilitate advanced applications such as human-machine interactions, human behavior analysis, active and assisted living, virtual and augmented reality, as well as ambient intelligence. However, recognizing hand gestures poses significant challenges due to the intricate nature of the human hand, which can assume countless poses and the wide variations in size and color across individuals. Furthermore, HGR applications frequently function in challenging settings marked by occlusions, changing backgrounds, noisy data, and demands for real-time processing.

A successful HGR framework needs to navigate the complexities introduced by the human hand and the application setting to satisfy both developers and end-users. Key performance indicators encompass ease of use, computational demand, hardware needs, response time, and accuracy. Hand gestures, inherently dynamic with poses and positions changing over time, introduce a temporal dimension to the recognition task.

Consequently, a sequence of hand poses must be interpreted to understand the meaning of a gesture. This paper presents a new approach which combines data-level fusion techniques with a specialized multi-stream CNN architecture, setting our method apart in addressing the challenges of dynamic gesture recognition.

Within the HGR domain, a variety of frameworks have been investigated, each focusing on different combinations of network architectures and input modalities to overcome specific challenges with dynamic gesture recognition. Certain frameworks enhance their performance by merging various input types, including RGB, skeleton data, optical flow, and depth maps, with different network architectures [1]–[8]. These multi-stream networks consist of various sub-networks designed with distinct input channels operating concurrently, with the features extracted from each sub-network merged to produce the final output of the overall network. On the other hand, multimodal networks process different input modalities through either distinct inputs in a multi-stream network or a combined input in a single-stream network. Also, several frameworks employ deep, data-driven neural network architectures, such as Recurrent Neural Networks (RNN) [1], [2], [9], [10], 3D Convolutional Neural Networks (3DCNN) [3], [6], [7], Attention Networks [2], [11], [12], and Long-Term Recurrent Convolutional Networks (LRCN) [13]–[15] to extract temporal information from dynamic hand gestures.

When developing real-world applications beyond the scope of academic research, it's important to focus on creating practical HGR-based systems. The developed frameworks often prioritize maximizing performance, which can lead to additional hardware demands, increased computational complexity and specialized, often expensive, sensors for input modalities. These factors, particularly with multimodal networks, can lead to higher costs, reduced user-friendliness, and longer inference times in real-time applications. Additionally, these frameworks require significant training data with data augmentation to attain acceptable levels of gesture recognition performance.

Skeleton-based HGR frameworks address these challenges by using data-level fusion to transform dynamic gesture data into RGB images. This method, which redefines gesture recognition as a standard image classification issue, has its own set of limitations. The implementation of data-level fusion in [16] results in noisy and visually similar RGB images which complicates gesture recognition and classification during model training and inference with their vanilla CNN architecture. In addition, the effectiveness of the selected view

Oluwaleke Yusuf and Maki Habib are with The American University in Cairo (AUC), Egypt. (e-mail: oluwaleke.umar, maki@aucegypt.edu)

Mohamed Moustafa was with The American University in Cairo (AUC), Egypt. He is now with Amazon, Seattle, USA. (e-mail: moustafa@ieee.org)

orientations is heavily dependent on how the skeleton data was initially captured. It is also worth noting that the framework has not been benchmarked against widely recognized HGR datasets, raising doubts about its performance relative to other frameworks.

This paper presents an effective data-level fusion and specialized CNN architecture for a robust, lightweight, skeleton-based HGR framework. The contributions of this paper include the following:

- 1) We enhance the conversion of 3D skeleton data to spatiotemporal 2D representational images for effective dynamic gesture recognition. This outcome is achieved using data-level fusion, incorporating denoising, and sequence fitting.
- 2) We introduce a simplified, fully-trainable Ensemble Tuner multi-stream CNN architecture for establishing robust semantic connections between multiple representations of the same input data during image classification.
- 3) We introduce a dynamic HGR framework aimed at minimizing hardware needs and computational complexity for HGR tasks, achieving parity with state-of-the-art (SOTA) benchmarks across various datasets.
- 4) We showcase our framework’s real-world applicability by developing a HGR application that satisfies real-time constraints and is compatible with standard consumer PC hardware.

Extensive experiments were conducted on five publicly available datasets: 3D Hand Gesture Recognition Using a Depth and Skeleton Dataset (SHREC2017) [17], Dynamic Hand Gesture 14/28 Dataset (DHG1428) [18], First-Person Hand Action Benchmark (FHPA) [19], Leap Motion Dynamic Hand Gesture Benchmark (LMDHG) [20], and Consiglio Nazionale delle Ricerche Hand Gestures Dataset (CNR) [16]. The outcomes indicate that our framework achieved performance closely aligned with, and in some instances surpassing, the state-of-the-art, with accuracies ranging from -4.10% to +6.86% compared to the highest benchmarks. Furthermore, the low latency of the HGR application successfully demonstrated the viability of data-level fusion for practical, real-time HGR applications. We also conducted an exploratory study using the SBU Kinect Interaction Dataset (SBUKID) [21] to investigate potential extensions of our framework for Human Action Recognition (HAR). The findings provide strong motivation for further development and experimentation.

The rest of this paper is structured as follows: **Section II** reviews the relevant HGR literature on skeleton modality, data-level fusion, and multi-stream architectures; **Section III** details the proposed HGR framework and associated methodologies; **Section IV** reports experimental findings and analyses using benchmark datasets; **Section V** describes the implementation of the HGR application; and **Section VI** concludes the paper and outlines avenues for future research.

II. RELATED WORK

This section provides an overview of significant research in the HGR domain, crucial for understanding the foundational

principles of our proposed framework. These works can be categorized into three approaches: recognition of hand gestures via skeleton data, data-level fusion of temporal information at the data level, and architectures based on multi-stream networks.

A. Skeleton-based Hand Gesture Recognition

Historically, HGR frameworks primarily relied on RGB videos or depth maps. However, with the evolution of technology and the emergence of a deeper understanding of gesture complexities, recent frameworks have shifted towards using skeleton poses as an input modality. This modality, usually derived from raw color and depth (RGB-D) data, provides a robust representation of hand positions and is effective at addressing issues like occlusions, variable backgrounds, and differences in individual hand morphologies. However, skeleton-based methods have the drawback of needing offline preprocessing to extract skeleton data from RGB-D sources, with a susceptibility to errors in this inferred data. Various methods for processing skeleton data have been developed within HGR frameworks.

Some significant contributions in this domain include: [22] utilized a Temporal Convolutional Network with a motion summarization module for processing skeleton pose features. [12] proposed a spatial-temporal attention network that relies on attention mechanisms to model inter-joint spatiotemporal dependencies, without requiring knowledge of joint positions or connections. [4] tackled skeleton data challenges by streamlining input features and the network design, using a network with Joint Collection Distances and global motion features at two scales. In [10], a Deep Convolutional LSTM (ConvLSTM) model was introduced, designed to inherently learn discriminative spatiotemporal features from skeleton data by capturing gestures across different scales.

Unimodal skeleton-based HGR frameworks consistently yield the best results [2], [12], [22]. Said frameworks not only show better performance with respect to computational efficiency metrics (like trainable parameters and FLOPS) but also network architectural complexity [2], [4], [12], [23]–[25]. Our proposed framework capitalizes on the robust encoding capabilities of the skeleton modality, towards achieving SOTA performance. Concurrently, we devised strategies to bypass the necessity for specialized hardware and high computational demands often associated with other skeleton-based approaches. Additionally, it is worth noting that skeleton-based HGR applications inherently reduce ethical concerns related to surveillance and privacy breaches, given the limited user-identifiable information in skeleton data [26], [27].

B. Data-Level Fusion

The challenges associated with recognizing dynamic hand gestures arise from their temporal attributes. Hand gestures are composed of a sequence of hand poses over time, necessitating an HGR framework capable of understanding the semantic connections between these successive poses for precise gesture identification. This complexity increases in multi-stream and

multimodal networks, which require precise pixel-level correspondence across various streams and modalities to recognize that the different inputs correspond to different representations of the same gesture sequence.

The effectiveness of the HGR framework is heavily influenced by the selected method for integrating input modalities and network streams. Deep Learning (DL) models typically implement fusion at the data-, feature-, or decision-level, each with distinct approaches [28]. HGR frameworks commonly utilize online decision-level and feature-level fusion, which affects performance differently. Such frameworks also demand complex network architectures, substantial training datasets (including data augmentation), and tailored loss functions to automatically align semantic and pixel-level details during training.

Temporal Information Condensation is a preprocessing technique used offline to convert spatiotemporal data from gesture sequences into static images before model training. This method of data-level fusion simultaneously captures the spatiotemporal variation of dynamic gestures, helping to resolve challenges related to spatiotemporal semantic coherence within multi-stream networks during training. By transforming the dynamic HGR task into a static image classification problem, this strategy enables the use of transfer learning with pre-trained models from well-known CNN architectures [16], [28].

In [28], Motion Fused Frames were introduced, where frames derived from optical flow serve as supplementary channels to static RGB images. Said optical flow frames, calculated from frames preceding the selected static image, are then processed using a Temporal Segment Network that employs a pretrained Inception CNN architecture. [29] describes a technique called star RGB, which transforms dynamic gestures from videos into single RGB images by summing the intensity differences of consecutive video frames. These images are then classified by a dynamic gesture classifier that uses an ensemble of ResNet CNNs fused via a soft-attention mechanism.

In [16], the authors exclusively used skeleton data to transform gesture information into RGB images, showcasing variations in hand joint positions during gestures on a plane. Temporal details are depicted through the color intensity of these projected points. Said images are subsequently classified using a pretrained ResNet-50 CNN, demonstrating effective performance on the balanced CNR dataset also developed by the authors. While promising, this approach could be further enhanced by refining the temporal information condensation method and network architecture for application to more challenging datasets

C. Multi-Stream Network Architectures

In developing advanced HGR frame, numerous high-performing frameworks adopt multi-stream network architectures that integrate decoupled spatiotemporal streams, operate on multiple temporal scales, and handle various input modalities. The goal of this strategy is to capture a wide range of contextual details from gesture sequences throughout the model’s training phase [6], [12], [22], [30]–[32]. The

effectiveness of this approach is evident as it provides the model with several ‘views.’ Such views enhance the model’s ability to distinguish between gestures that may appear similar and reduces the likelihood of overfitting. Nevertheless, multi-stream networks depend on the integration of features at two specific levels: the combination of features from different convolutional layers (feature-level fusion), and the merging of classification probabilities from the network’s dense layers (decision-level fusion). These fusion techniques are crucial for compiling and balancing the contributions from each sub-network, thereby improving the overall network’s functionality.

To identify and categorize continuous hand gestures, [6] employed a hierarchical architecture comprising two models of 3D-CNNs. Initially, a detector model spots a gesture within the video frames and subsequently triggers a deeper classifier model which further hones the detector’s findings to classify the gestures accurately. Diverging from approaches that blend multimodal data, [30] employed unique I3D sub-networks to process information from different modalities. These sub-networks maintain a stable correlation throughout their deeper levels, using spatiotemporal semantic alignment loss to ensure feature coherence across the networks. [31] developed a multi-channel CNN consisting of separate feature extraction modules for high-resolution and low-resolution channels, coupled with a dedicated residual branch per channel. Skeleton sequences are initially resized and then broken down into unidimensional joint sequences, which are then inputted into the corresponding channel of the model.

Frameworks that utilize data-level fusion tend to adopt either a straightforward single-stream CNN architecture [16] or a two-stream CNN architecture with features concatenated at the feature level [28]. Conversely, [29] implemented a novel soft-attention mechanism for feature-level fusion, leading to a slight boost in classification accuracy over other fusion methods. This indicates a knowledge gap concerning network architectures specially engineered for processing spatiotemporal images generated via data-level fusion. Furthermore, the fusion techniques employed at both feature and decision levels in multi-stream frameworks can be refined to enhance semantic alignment and minimize computational overhead.

III. HAND GESTURE RECOGNITION FRAMEWORK

This section elaborates on the essential elements of the proposed skeleton-based hand gesture recognition framework shown in Figure 1. Initially, the technique of temporal information condensation for generating static, spatiotemporal RGB images is explored. Subsequently, the network architecture that takes advantage of this data-level fusion strategy is introduced. Finally, the data-level fusion and network architecture are merged to present an HGR framework adaptable to any source of hand skeleton data—real-time inference or collated datasets.

A. Data-Level Fusion

Data-level fusion serves as an initial processing stage, conducted either offline or online, where data from the spatial and temporal channels of a dynamic gesture sequence are merged

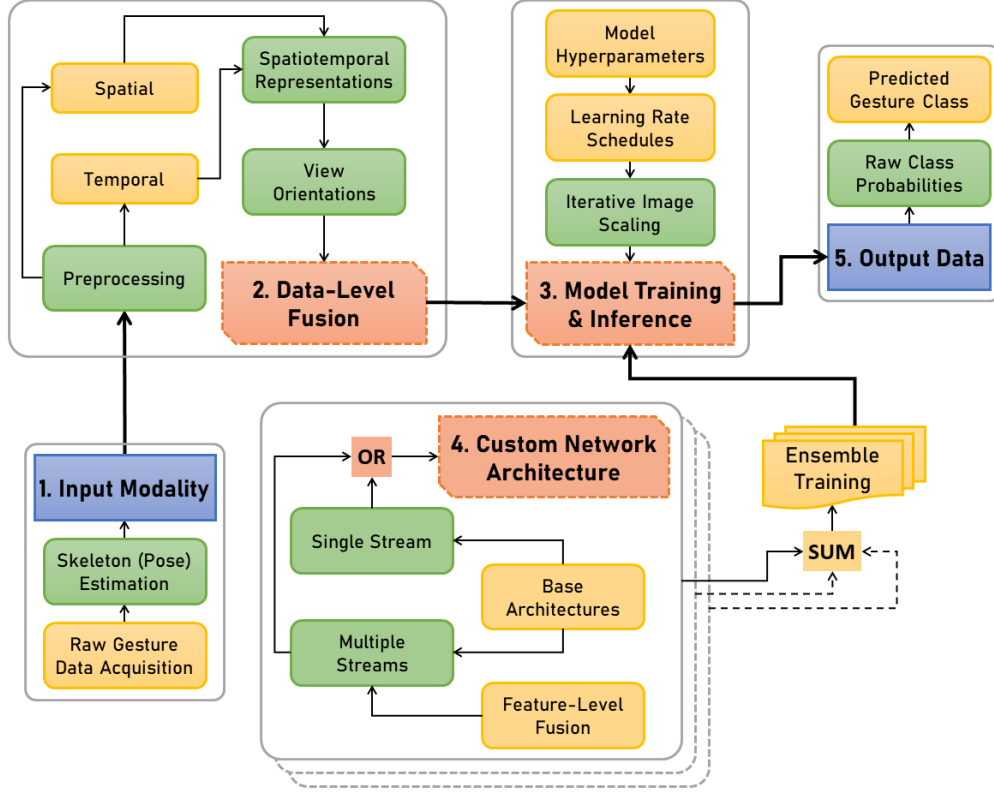


Fig. 1. Diagrammatic Overview of the Proposed HGR Framework [33], Highlighting Key Components for Recognizing and Classifying Dynamic Hand Gestures.

into a static 2D spatiotemporal image, preserving a square aspect ratio. This transformation involves condensing the temporal information present in the original sequence while retaining pertinent semantic information about the gesture. Similar to the approach in [33], the problem of transforming a dynamic gesture sequence into a static spatiotemporal image can be defined as follows:

Let g_i denote a dynamic gesture, and let $S = C_{h,h=1}^N$ represent the set of gesture sequences across N classes. The temporal variation of g_i is defined in Equation 1 as follows:

$$G_i = \{G_i^\tau\}_{\tau=1}^{T_i} \quad (1)$$

In the context of a temporal window sized T_i , $\tau \in [1, T_i]$ specifies a precise moment τ , and G_i^τ indicates the frame of g_i at that moment. The challenge of classifying dynamic hand gestures involves assigning the correct class C_h for sequence g_i .

Gesture sequences in the set S present varying lengths of time windows based on the gesture category and the performer's execution. Each sequence g_i in S is resampled to a uniform temporal window T_i , set to be longer than any existing window T_i in S . This adjustment has the following effects on each gesture sequence g_i :

- It smoothens out inaccuracies in individual frames G_i^τ arising during pose estimation.

- It minimizes minor variances in motion paths and sequence durations that result from the unique way each person performs a gesture.

In combination, the resampling adjustment underscores the commonalities between gesture sequences $g_i \in C_h$ in S , thereby improving the condensation of temporal information, consequently improving the model's accuracy when classifying gestures. Each resampled gesture g_i is then split into its spatial and temporal components as follows:

- **Spatial:** This component encodes changes in hand pose across each frame G_i^τ as a 3D model of the hand's skeleton. Each finger is shown in a distinct CSS color, selected to provide strong contrast with the other colors in the and the dark background.
- **Temporal:** In this channel, hand movement is encoded through 3D visualizations of "temporal trails" of the five fingertips, extending from the start of the gesture G_i^1 to its end G_i^T . These trails comprise a sequence of markers, with distinct CSS colors correlating to their respective fingers. The transparency of these markers, indicated by the alpha channel, varies over time, making markers from earlier in the sequence ($\tau \approx 1$) more transparent, and those closer to the end ($\tau \approx T$) more opaque, thus capturing the temporal dynamics.

Temporal information condensation creates, for each resampled gesture g_i , a 3D spatiotemporal image, which merges the hand pose at last frame G_i^T with the temporal path it has

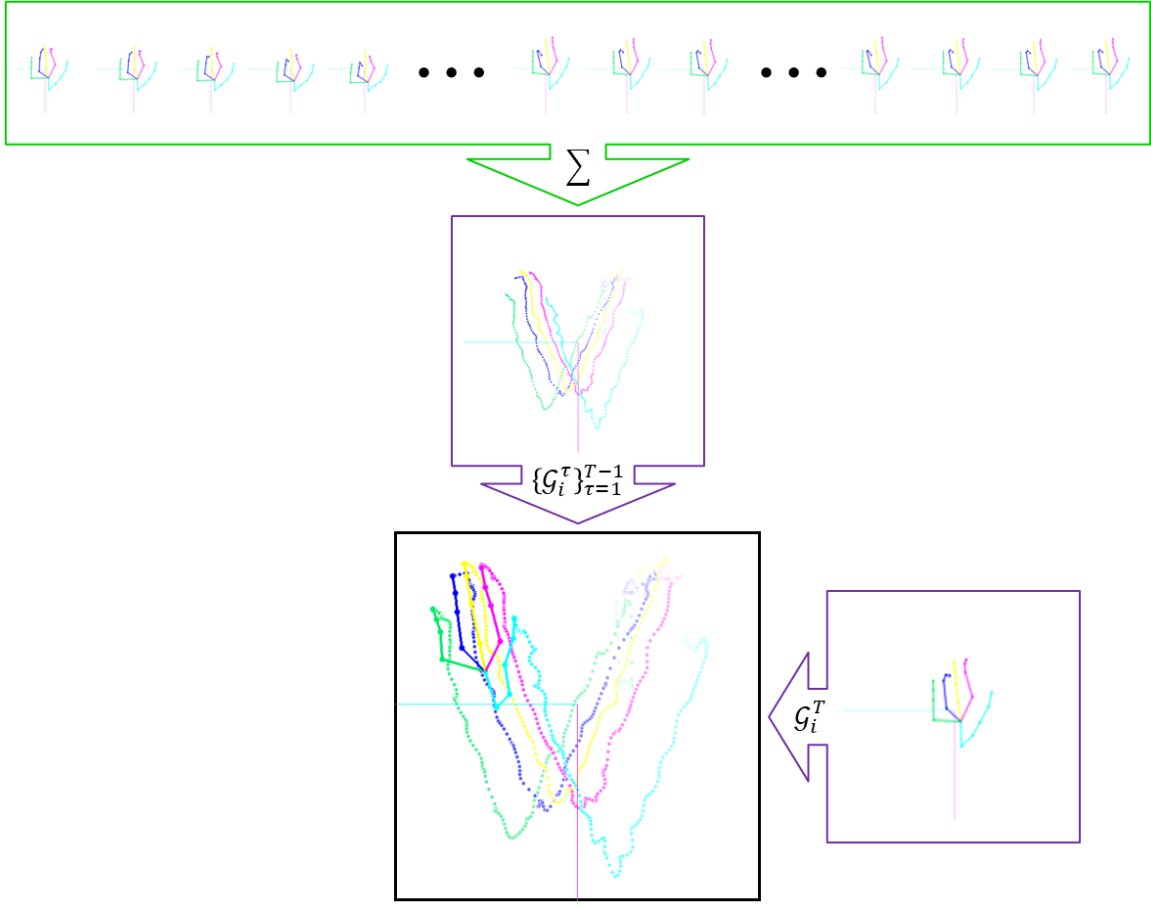


Fig. 2. Workflow of Data-Level Fusion: Illustrating the Transformation of 3D Skeleton Data into 2D Spatiotemporal RGB Representations for Image Classification.

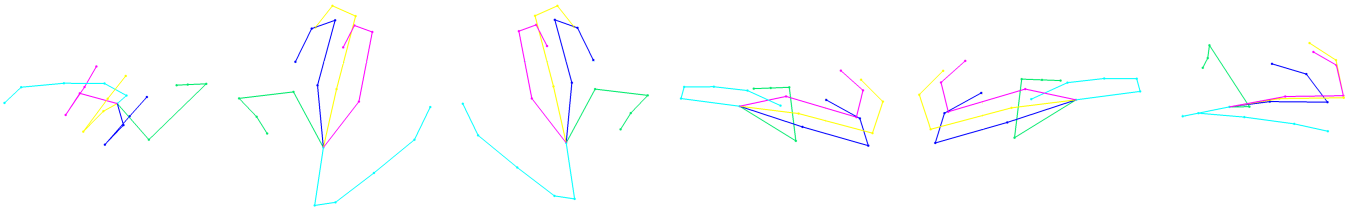


Fig. 3. Illustration of View Orientations Used for Spatiotemporal Gesture Representations. Left-to-Right: Top-Down, Front-To, Front-Away, Side-Right, Side-Left, and Axonometric.

followed $G_i^T_{\tau=1}^{T-1}$, as illustrated in Figure 2. The 3D spatiotemporal image can be viewed from any arbitrary perspective (view orientation). This paper considers six (6) specific view orientations (VOs)—axonometric, front-away, side-left, top-down, front-to, and side-right. These VOs are defined by the elevation and azimuth angles set for the virtual camera during the visualization process, detailed in Figure 3. The choice of angles differs across datasets, influenced by the methods used to collect and derive skeleton data from the actual gestures by participants.

The outcome of the data-level fusion for any given gesture g_i is a single image of the 3D spatiotemporal representation from one of the chosen view orientations VO_j where $j \in [1, 6]$. Adjustments to the virtual camera's zoom level and

position are essential during visualization to ensure that the spatiotemporal representation is fully enclosed within the static image without being cropped off or any truncation. These settings cannot be manually set or fixed, as they fluctuate for every gesture g_i , and set of sequences S . Instead, the sequence fitting for each gesture g_i is estimated as follows:

$$g_i = g_i - \text{mean}(g_i) - (L/2) \quad (2)$$

$$P = (L/2) \quad (3)$$

$$Z_i = \max(g_i) - \min(g_i) + \gamma \quad (4)$$

Equation 2 represents the adjustment made to each gesture g_i to fit it within the static image. By subtracting the mean of the gesture from itself and subtracting half of the length L of the static image, the gesture is shifted to the center of the image. The adjustment made in Equation 2 ensures that the virtual camera can be fixed to position P in 3D space, which coincides with the center of the static image for all $g_i \in S$. As outlined in Equation 3, the value of P is determined by the length L of the static image. Equation 4 calculates the zoom level Z_i of the virtual camera for each gesture g_i . The zoom level is estimated from the bounds of the gesture’s representation, with an optional padding value γ for tweaking the estimated zoom level for all $g_i \in S$. With the full extent of the gesture taken into account, the zoom level ensures that the entire spatiotemporal representation remains visible in the image without being cropped off.

In conclusion, the data-level fusion transforms the dynamic hand gesture classification task into a static image classification problem task. Thus, by employing a mapping function Φ , the 3D skeleton information of a dynamic gesture g_i from any view orientation VO_j is transformed into a single 2D spatiotemporal image $I_{ij} = \Phi(G_i)$. This image becomes the input for the classification task, where the goal is to determine the correct class C_h for I_{ij} . This approach simplifies the classification problem by leveraging established techniques in image classification, enabling the utilization of existing research and algorithms in this domain.

B. Ensemble Tuner Multi-Stream CNN Architecture

With the set S , consisting of dynamic hand gestures g_i , converted into static spatiotemporal images I_{ij} , traditional CNN architectures become suitable for classifying these gestures. The HGR framework also take advantage of transfer learning by using models from deep learning CNN architectures that were originally developed for image classification. Transfer learning enables swift convergence during model training and expedites prototype development within the framework. To choose the base architecture for our network, we evaluated several CNN models pretrained on the ImageNet dataset, which have demonstrated state-of-the-art (SOTA) performance.

During transfer learning, the pre-trained model’s fully-connected (FC) layers are customized to fit the new task at hand. We substituted the original FC layers with a tailored classifier, maintaining the primary convolutional layers (along with their pre-trained weights) to serve as an encoder. As depicted in Figure 4, this new classifier includes additional pooling, batch normalization, dropout, linear, and non-linear layers, all trained from scratch. This approach repurposes the feature maps extracted by the encoder more effectively for the new classification task. The classifier produces a set of probabilities, predicting the likelihood that the input image I_{ij} belongs to any class $C_h, h \in [1, N]$ within the set S .

To leverage the diverse view orientations available during data-level fusion for generating the spatiotemporal images, we employ the specialized multi-stream CNN architecture illustrated in Figure 5. This architecture, which utilizes transfer learning and ensemble training, is specifically engineered

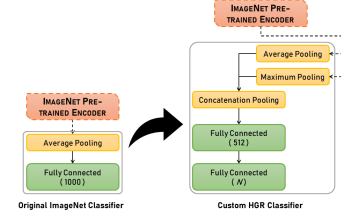


Fig. 4. Comparison of Classifiers: The Original ImageNet Classifier (left) versus Our Tailored HGR Classifier (right).

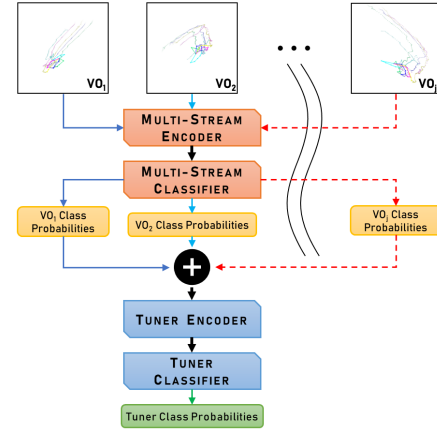


Fig. 5. Illustration Showing the Processing of Static Spatiotemporal Images by the Ensemble Tuner Multi-Stream CNN Architecture.

to process spatiotemporal images generated from any view orientation VO_j . For each gesture $g_i \in S$, data-level fusion produces a set of $I_{ij}^6_{j=1}$ spatiotemporal images, corresponding to j different view orientations.

Each image I_{ij} is sequentially input into the multi-stream encoder for feature extraction. The derived feature maps are then processed by the multi-stream classifier, as illustrated in Figure 4 (right), producing a series of class probabilities $\{CP\}_{ij(h=1)}^{h,N}$. The multi-stream encoder and classifier are shared across all images, effectively lowering the computational demands of the network architecture. However, a limitation of this approach is that the ordering of images (view orientations) is not random, resulting in an expanded search space for the ideal sequence. The multi-stream encoder and classifier sub-network jointly learn the best weights for merging the view orientations VO_j guided by loss calculated for each image I_{ij} . Given that each image yields a unique loss value, the sequence (order and combination) of the input spatiotemporal images affects the performance of the multi-stream sub-network [33].

The class probabilities $\{CP\}_{ij(h=1)}^{h,N}$ obtained from the multi-stream classifier are transformed into a single RGB pseudo-image via online decision-level fusion. This pseudo-image is then passed through into an ensemble tuner sub-network, producing another set of class probabilities. The tuner utilizes a comparatively simple, pre-trained CNN architecture as an encoder, whereas its classifier is unchanged as shown in Figure 4 (right). The ensemble tuner multi-stream CNN architecture undergoes end-to-end training, yielding $(j + 1)$

class probabilities and losses for each gesture g_i . Only the class probabilities—and classification accuracy—obtained from the ensemble tuner sub-network are reported in this paper. To tackle the multi-task nature of the problem, a specialized loss function inspired by [34] is employed. Similar to the approach outlined in [33], this loss function accounts for the homoscedastic uncertainties related to the view orientations and the ensemble tuner by appropriately weighing the $(j + 1)$ cross-entropy losses.

Implementing a multi-stream network that accepts inputs from diverse view orientations helps the model distinguish between gesture classes that look similar when visualized from a single view orientation, thus improving the classification accuracy. Additionally, using of RGB pseudo-images for decision-level fusion facilitates transfer learning and aids in preserving semantic alignment among the class probabilities $\{CP\}_j$ generated for each view orientation $\{VO\}_j$ by the multi-stream sub-network. Integrating the multi-stream and ensemble tuner sub-networks into a single architecture circumvents the need to train multiple models separately, addressing a common limitation of conventional ensemble training approaches.

IV. EXPERIMENTS & RESULTS

A. Datasets

In this section, we review the five benchmark datasets used in the experiments to build and test the main elements of our proposed HGR framework, along with its comparison to the current state-of-the-art (SOTA). Each dataset presents distinct challenges and opportunities for the development and evaluation of HGR frameworks.

- **CNR**: The CNR dataset [16] includes spatiotemporal images captured from a top-down view, covering 1925 gesture sequences across 16 classes. This dataset is split into a training set with 1348 images and a validation set with 577 images. The absence of raw skeleton data presents a limitation as our framework can only be trained from one viewpoint.
- **LMDHG**: Comprising 608 gesture sequences over 13 classes, the LMDHG dataset [20] is divided into training (414 gestures) and validation (194 gestures) sets. The dataset exhibits minimal overlap in subjects across both subsets, featuring comprehensive 3D skeleton data comprising a total of 46 hand joints for each hand.
- **FPHA**: This dataset [19], featuring a wide range of styles, viewpoints, and scenarios, includes 1175 gesture sequences across 45 classes. Its primary challenges stem from the similarity in motion patterns, the diverse range of objects involved, and a low ratio of gesture sequences to classes. The dataset is divided into 600 gestures for training and 575 for validation, providing 3D skeleton data for 21 hand joints per subject.
- **SHREC2017**: With 2800 sequences performed by 28 subjects, the SHREC2017 dataset [17] is designed for both coarse and fine-grained gesture classification, divided into 14-gesture (14G) and 28-gesture (28G) benchmarks. The dataset provides 3D skeleton data for 22 hand

joints and employs a 70:30 random-split protocol for the training (1960 gestures) and validation (840 gestures) subsets.

- **DHG1428**: Following a structure similar to SHREC2017, the DHG1428 dataset [18] comprises 2800 sequences performance by 20 subjects for the 14G and 28G benchmarks. It provides equivalent skeleton data and follows the same 70:30 split for training and validation.
- **SBUKID**: This smaller HAR dataset [21] contains 282 action sequences across eight classes involving two-person interaction. SBUKID provides skeleton data for 15 joints per subject and uses a five-fold cross-validation evaluation protocol, with average accuracies reported across all folds.

B. Generalized HGR Framework

Our proposed HGR framework, in its generalized form, incorporates data-level fusion to create static 2D spatiotemporal images combined with the ensemble tuner multi-stream CNN architecture for classifying said images. Table I shows that the elevation and azimuth angles of the virtual camera required for the view orientations during data-level fusion are dataset-specific. The same padding value $\gamma = 0.125$ was used for all datasets during sequence fitting. Note that the aforementioned settings do not apply to the CNR dataset as it only provides static images.

For the custom network architecture, the performance of 26 distinct CNN architectures from the ResNet, Inception, EfficientNet, ResNeXt, SE-ResNeXt, SE-ResNet, and xResNet families were evaluated as shown in Table II. Said architectures were pre-trained on ImageNet and trained with a dataset of static, spatiotemporal images generated from the DHG1428 dataset and front-to view orientation. From the empirical results for two distinct training setups (TS1 and TS2), the ResNet variants ResNet-50 and ResNet-18 were selected as the base encoders for our custom network architecture’s multi-stream and ensemble tuner sub-networks.

The optimal sequence of VOs for feeding spatiotemporal inputs into the multi-stream sub-network is specific to each dataset, depending on the specifics of how the raw gestures were collected and processed. Our experiments showed that combinations of three unique VOs are enough for good classification performance. We employed an iterative approach to determine the optimal sequence of VOs: initially, each VO was trained individually in a single-stream network. Then, paired combinations of the highest-performing VOs were trained in a two-stream network. Following this, triple combinations of the top-performing VO pairs were trained in a three-stream network. This process identifies the optimal sequence of three VOs tailored to each dataset.

C. Implementation and Training

The developed framework was developed using Python 3.8.5, and tested on a Linux Ubuntu 18.04 server with four NVIDIA GeForce GTX TITAN X graphics cards. For data-level fusion, the **Vispy** visualization library was utilized, whereas **OpenCV** was employed to generate pseudo-images

TABLE I
VIRTUAL CAMERA (ELEVATION, AZIMUTH) ANGLES (IN DEGREES) FOR EACH VIEW ORIENTATION.

View Orientation	DHG1428	SHREC2017	FHPA	LMDHG
top-down	(0.0, 0.0)	(0.0, 0.0)	(90.0, 0.0)	(0.0, 0.0)
front-to	(90.0, 180.0)	(90.0, 180.0)	(0.0, 180.0)	(-90.0, -180.0)
front-away	(-90.0, 0.0)	(-90.0, 0.0)	(0.0, 0.0)	(90.0, 0.0)
side-right	(0.0, -90.0)	(0.0, -90.0)	(0.0, 90.0)	(0.0, 90.0)
side-left	(0.0, 90.0)	(0.0, 90.0)	(0.0, -90.0)	(0.0, -90.0)
custom	(30.0, -132.5)	(30.0, -132.5)	(25.0, 115.0)	(-15.0, -135.0)

TABLE II
COMPARATIVE ANALYSIS OF VARIOUS PRE-TRAINED CNN ARCHITECTURES.

CNN Architecture		Classification Accuracies (%)		
Family	Variants	TS1	TS2	Average
ResNet	ResNet18	0.8083	0.7762	0.8149
	ResNet34	0.8190	0.7952	
	ResNet50	0.8417	0.8012	
	ResNet101	0.8226	0.8286	
	ResNet152	0.8310	0.8250	
Inception	Inception-v3	0.8155	0.7762	0.8124
	Inception-v4	0.8310	0.7964	
	Inception-ResNet-v1	0.8179	0.8262	
	Inception-ResNet-v2	0.8167	0.8190	
EfficientNet	EfficientNet-B0	0.8143	0.7964	0.8083
	EfficientNet-B3	0.8107	0.8107	
	EfficientNet-B5*	0.8143	0.8131	
	EfficientNet-B7*	0.7893	0.8179	
ResNeXt	ResNeXt26	0.8048	0.7726	0.8042
	ResNeXt50	0.8298	0.7952	
	ResNeXt101	0.8226	0.8000	
SE-ResNeXt	SE-ResNeXt50	0.8143	0.7595	0.8033
	SE-ResNeXt101	0.8405	0.7988	
SE-ResNet	SE-ResNet18	0.7881	0.7774	0.8032
	SE-ResNet26	0.8048	0.7726	
	SE-ResNet50	0.8179	0.8024	
	SE-ResNet101	0.8310	0.8131	
	SE-ResNet152	0.8060	0.8190	
xResNet	xResNet50	0.7440	0.7333	0.7379
	xResNet50-Deep	0.7226	0.7357	
	xResNet50-Deeper	0.7405	0.7512	

for decision-level fusion. Furthermore, the entire machine learning workflow, including the design of network architectures and the training of models, was carried out using **PyTorch** and **FastAI**. The code for this paper can be found at [this GitHub repository](#).

During data-level fusion, each gesture sequence was re-sampled to a unified temporal window $T = 250$ frames. The static images and pseudo-images were generated with a square aspect ratio at 960px and 224px respectively. During the training phase, a batch size of 16 was utilized, the Adam optimizer was employed, and a custom loss function incorporating cross-entropy and homoscedasticity was applied. The training was conducted in multiple stages, with the dimensions of the static input images progressively adjusted to 224px, 276px, 328px, and 380px (as needed) to enhance model performance. The cosine annealing schedule was utilized for

the learning rate, and the initial learning rate for each stage was automatically determined using the FastAI `learner.lr_find` method. Furthermore, various data augmentation techniques were applied during the training process, including random horizontal flips, affine transformations, perspective warping, random zooms, random rotations, and adjustments in color space.

D. Results on the CNR Dataset

Table III presents a comparative evaluation of our proposed framework with other HGR frameworks on the CNR dataset. Our proposed framework exhibited slightly lower performance compared to the SOTA [16] by -1.73%. This drop in performance can be attributed to the absence of raw skeleton data for data-level fusion. Thus, our enhanced data-level fusion—which incorporates denoising, sequence fitting, and multiple view orientations—was not available during model training.

TABLE III
COMPARISON OF VALIDATION ACCURACY WITH SOTA ON THE CNR DATASET

Method	Classification Accuracy (%)
Proposed Framework	97.05
Lupinetti et al. [16]	98.78

E. Results on the LMDHG Dataset

Table IV provides a comparative performance analysis between our proposed framework and other HGR frameworks on the LMDHG dataset. Our framework surpassed the SOTA results presented in [16] by +6.86%, attributed to the utilization of our improved data-level fusion approach for generating spatiotemporal images. These evaluation results highlight the effectiveness of our data-level fusion enhancements and the subsequent shift from dynamic hand gesture recognition to static image classification. In addition, our transformation process effectively preserved crucial semantic information by utilizing an optimal sequence of view orientations—[custom, front-away, top-down].

F. Results on the FPHA Dataset

As previously mentioned, the FPHA dataset is quite challenging for HGR evaluation, and this difficulty is further exacerbated by the adoption of a 1:1 evaluation protocol,

TABLE IV
COMPARISON OF VALIDATION ACCURACY WITH SOTA ON THE LMDHG DATASET

Method	Classification Accuracy (%)
Boulahia et al. [20]	84.78
Lupinetti et al. [16]	92.11
Mohammed et al. [10]	93.81
Proposed Framework	98.97

resulting in closely balanced training and validation proportions. Table V presents our proposed framework’s performance compared to other HGR frameworks evaluated on the FPHA dataset. Employing an optimal sequence of view orientations—[front-away, custom, top-down]—our proposed framework fell short of the SOTA [22] by -4.10%.

TABLE V
COMPARISON OF VALIDATION ACCURACY WITH SOTA ON THE FPHA DATASET

Method	Classification Accuracy (%)
Sahbi [35]	86.78
Liu et al. [11]	89.04
Li et al. [2]	90.26
Liu et al. [3]	90.96
Proposed Framework	91.83
Nguyen et al. [36]	93.22
Rehan et al. [32]	93.91
Sabater et al. [22]	95.93

G. Results on the SHREC2017 Dataset

Table VI presents a comparative analysis between our proposed framework and other HGR frameworks on the SHREC2017 dataset. The empirically established ideal sequence of view orientations, [front-away, custom, front-to], resulted in 14G and 28G validation accuracies of 97.86% and 95.36%, respectively. These results show improvements of +0.86% and +1.46% in comparison to the SOTA results reported in [12].

TABLE VI
COMPARISON OF VALIDATION ACCURACY WITH SOTA ON THE SHREC2017 DATASET

Method	Classification Accuracy (%)		
	14G	28G	Average
Sabater et al. [22]	93.57	91.43	92.50
Chen et al. [37]	94.40	90.70	92.55
Yang et al. [4]	94.60	91.90	93.25
Liu et al. [3]	94.88	92.26	93.57
Liu et al. [11]	95.00	92.86	93.93
Rehan et al. [32]	95.60	92.74	94.17
Mohammed et al. [10]	95.60	93.10	94.35
Deng et al. [23]	96.40	93.30	94.85
Min et al. [9]	95.90	94.70	95.30
Shi et al. [12]	97.00	93.90	95.45
Proposed Framework	97.86	95.36	96.61

H. Results on the DHG1428 Dataset

Table VII showcases an extensive evaluation of our proposed framework with other HGR frameworks on the DHG1428 dataset. Employing the optimal sequence of view orientations—[custom, top-down, front-away]—the 14G and 28G validation accuracies were 95.83% and 92.38%, respectively. Thus, our framework exhibited a marginally lower performance than the SOTA [2] by -0.48% and -1.67%, respectively.

TABLE VII
COMPARISON OF VALIDATION ACCURACY WITH SOTA ON THE DHG1428 DATASET

Method	Classification Accuracy (%)		
	14G	28G	Average
Lai et al. [38]	85.46	74.19	79.83
Chen et al. [39]	84.68	80.32	82.50
Weng et al. [40]	85.80	80.20	83.00
Devineau et al. [31]	91.28	84.35	87.82
Nguyen et al. [36]	92.38	86.31	89.35
Chen et al. [37]	91.90	88.00	89.95
Mohammed et al. [10]	91.64	89.46	90.55
Liu et al. [3]	92.54	88.86	90.70
Liu et al. [11]	92.71	89.15	90.93
Nguyen et al. [41]	94.29	89.40	91.85
Shi et al. [12]	93.80	90.90	92.35
Proposed Framework	95.83	92.38	94.11
Li et al. [2]	96.31	94.05	95.18

It is important to acknowledge that while the SHREC2017 and DHG1428 datasets share similarities, DHG1428 offers a more equitable distribution of subjects across all classes. Consequently, the DHG1428 14G and 28G classification accuracies reported by HGR frameworks tend to be consistently lower than those reported for the SHREC2017 dataset [3], [11], [12], [37]. In this regard, our proposed framework did not deviate from this trend, with DHG1428 14G and 28G results -2.03% and -2.98% lower than their SHREC2017 equivalents.

Figure 6 presents the confusion matrix of our framework’s performance on the DHG1428 28G dataset. As evident from the robust validation accuracy of 92.38%, a significant alignment exists between the actual gesture classes and their corresponding predictions. Note that class labels in the figure are augmented with numerical prefixes, differentiating between the DHG1428 performance modes. The prefixes specifically denote whether the gesture was executed with one finger (01-14) or the entire hand (15-28).

Consistent with the observations in previous research observations [42], our analysis underscores a significant challenge in differentiating between the “Grab” and “Pinch” gesture classes. This challenge persists across both performance modes and becomes apparent when visually inspecting the images generated for these two gesture classes. The visual similarity between them is significant enough to cause confusion even for human observers.

I. Ablation Study on SBUKID Dataset

Due to the design of the data-level fusion process, we believe our proposed framework is domain-agnostic and is similarly applicable to other domains involving the classification of

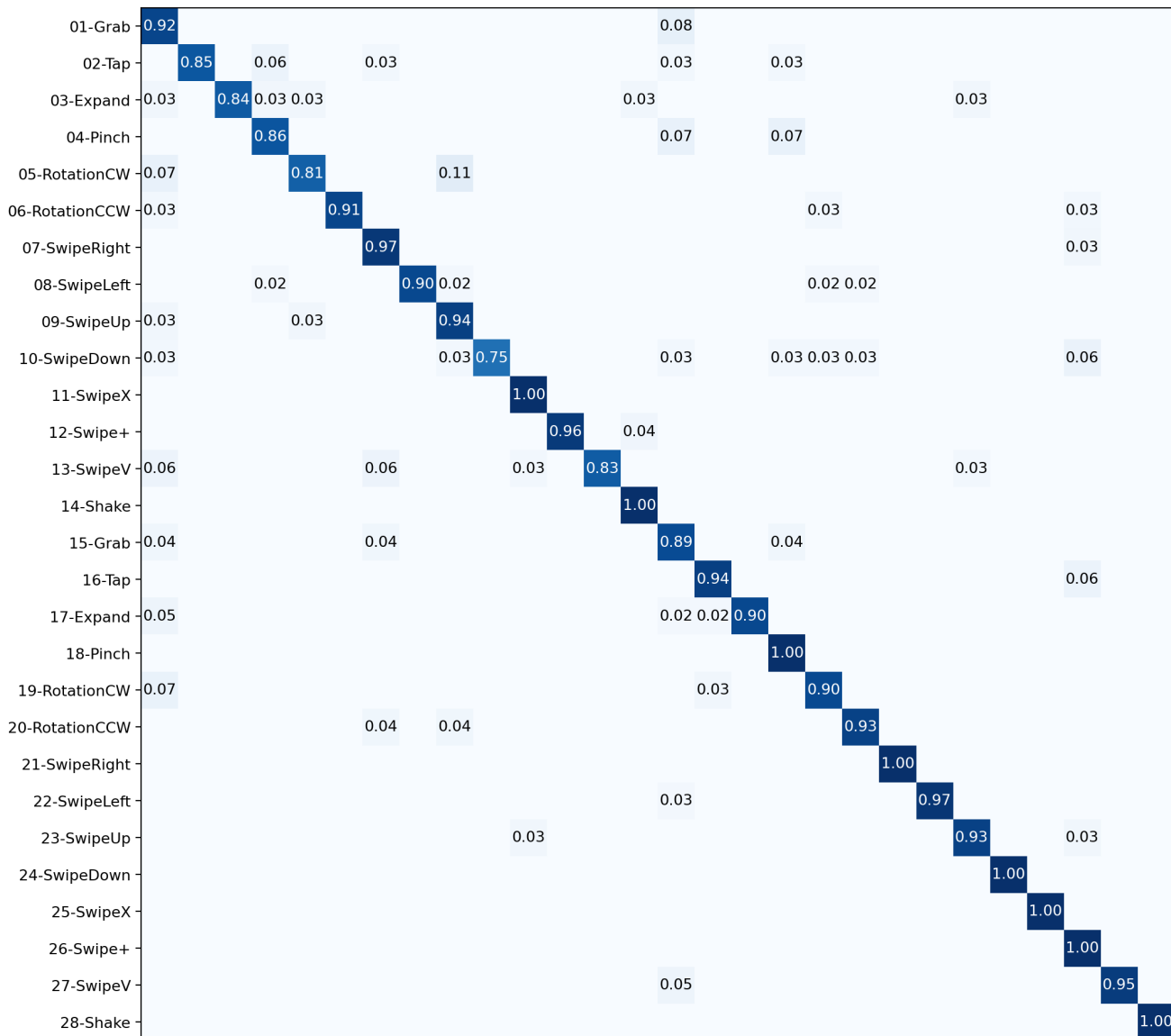


Fig. 6. Confusion Matrix for the Proposed Framework on the DHG1428 28G Dataset.

temporal dynamic data in the form of 2D/3D coordinates. To test this hypothesis, we adapted our framework to the skeleton-based Human Action Recognition (HAR) domain, with slight alterations in the data-level fusion process. HAR, similar to HGR, enables computers to recognize and interpret dynamic human actions by using the entire human body as input.

We utilized the SBUKID dataset to create spatiotemporal datasets visualized from all six view orientations. Each dataset was then independently used to train a custom single-stream CNN architecture based on a pre-trained ResNet-50 encoder. From the experimental results in Table VIII, our proposed framework compares favorably with other specialized HAR frameworks, achieving an average cross-validation classification accuracy of 93.96% with the single [front-away] view orientation. Without utilizing the specialized e2eET multi-stream CNN architecture, said performance is only -4.34% lower than the SOTA, thus highlighting the effectiveness of our data-level fusion design for transforming temporal dynamic

data from various domains for image classification.

TABLE VIII
COMPARISON OF VALIDATION ACCURACY WITH SOTA ON THE SBUKID DATASET

Method	Average Cross-Validation Classification Accuracy (%)
Song et al. [43]	91.50
Liu et al. [44]	93.50
Kacem et al. [45]	93.70
Proposed Framework	93.96
Ke et al. [46]	94.17
Liu et al. [47]	94.90
Maghoumi et al. [48]	95.70
Zhang et al. [49]	98.30

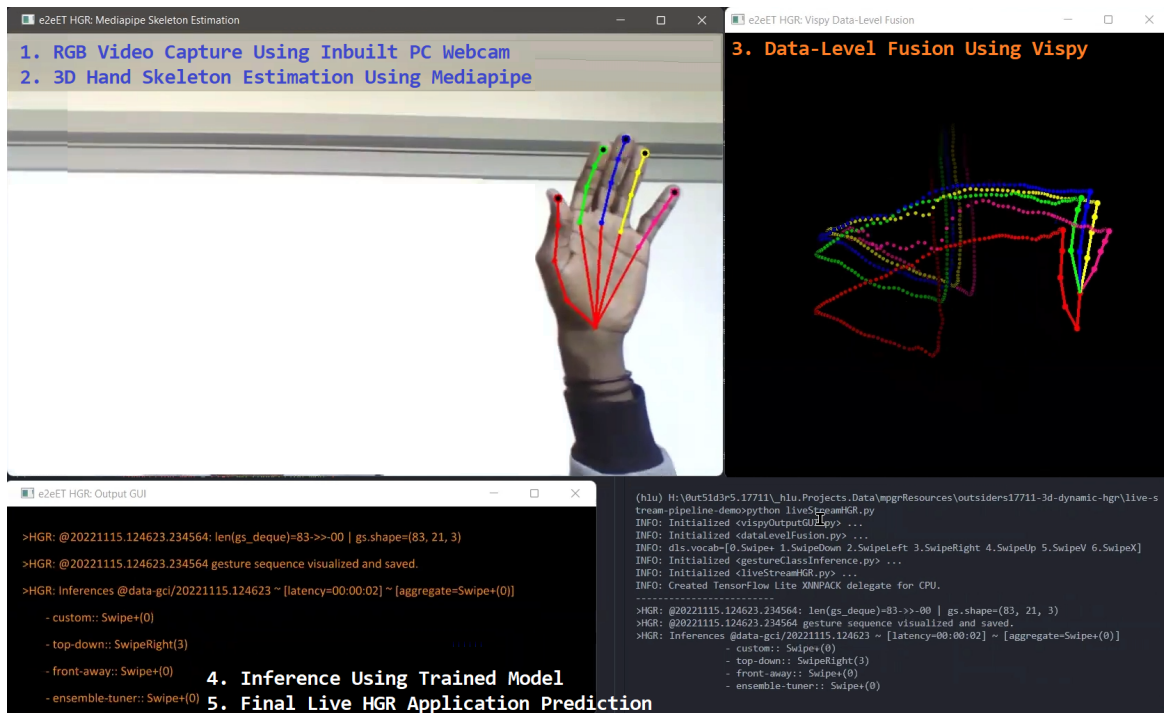


Fig. 7. Demonstration of the Real-Time HGR Application, Based on Our Proposed Dynamic HGR Framework.

V. REAL-TIME HGR APPLICATION

To demonstrate the practical utility of our proposed framework in reducing hardware and computational demands for HGR-based applications, we developed a real-time HGR application [33] based on our generalized HGR framework. This application’s underlying model was trained specifically on the “Swipe” gestures from the DHG1428 dataset, including gestures like “Up”, “Down”, “Right”, “Left”, “+”, “V”, and “X”. The operational pipeline of the application is depicted in Figure 7 and can be summarized as follows:

- 1) OpenCV captures the raw gesture data as RGB videos from the inbuilt PC webcam.
- 2) The video frames are processed for hand detection and pose estimation using **MediaPipe Hands**.
- 3) Data-level fusion is performed on the skeleton data, resulting in three spatiotemporal images from [custom, top-down, front-away] view orientations.
- 4) These spatiotemporal images are then processed by the trained DHG1428 model, which produces four class predictions: three from the multi-stream sub-network and one from the ensemble tuner sub-network.
- 5) An output graphical user interface (GUI) presents the class predictions, information about the input gesture sequence, and the framework’s latency.

The real-time application effectively showed that a standard PC webcam can adequately collect raw dynamic gesture data from a user, negating the necessity for extra specialized and costly sensors. On a PC equipped with an Intel Core i7-9750H CPU and 16GB of RAM, the application maintained a latency of 2-3 seconds with a capture rate of 15 frames per second from the execution of a gesture to the completion of model

inference. Compared with other applications running on the PC, the total CPU and RAM usage was deemed acceptable and had a negligible impact on the PC’s functionality and other applications running simultaneously.

VI. CONCLUSIONS AND FUTURE WORK

A. Conclusions

This paper first explores various frameworks for dynamic HGR and then introduces a robust framework for skeleton-based hand gesture recognition (HGR) that efficiently converts the task of recognizing dynamic hand gestures into that of static image classification while preserving essential semantic information. The framework incorporates an improved data-level fusion technique to generate static RGB spatiotemporal images from hand pose information. It also introduces an ensemble tuner multi-stream CNN architecture, which leverages multiple view orientations for accurate classification of the static images while maintaining computational efficiency.

Extensive experiments were conducted on five benchmark datasets to evaluate the effectiveness and generalization of the proposed HGR framework. The results demonstrate the framework’s competitiveness, achieving accuracies within a range of -4.10% to +6.86% compared to reported state-of-the-art validation accuracies. Ablation studies related to the human action recognition domain also yielded competitive results, falling -4.34% short of the reported state-of-the-art validation accuracy. These findings highlight the framework’s efficacy in handling temporal dynamic data across various domains.

Additionally, the framework’s practical usefulness was illustrated by creating a real-time HGR application. This application functioned using a standard built-in PC webcam and

showed low CPU and RAM resource consumption, highlighting its efficiency. This underscores the viability of data-level fusion in reducing hardware requirements and computational complexity without compromising latency and frames-per-second performance.

B. Future Work

In addition to the achievements outlined in this work, several potential enhancements and expansions could be explored in future research. Extending the approach to skeleton-based Human Action Recognition (HAR) is a natural progression. HGR and HAR exhibit sufficient similarities to justify leveraging the existing framework to recognize and categorize human actions based on skeletal data.

Another area worth exploring is enhancing the multi-stream network architecture. Integrating transformers or attention networks into the architecture has shown promise in improving performance. Given the advancements in attention mechanisms in deep learning, further exploration of their application to enhance hand gesture recognition and other tasks would be valuable.

Testing the implementation of the developed framework in real-world scenarios is crucial to validate its practicality. Deploying the framework in domains like healthcare or virtual reality can provide valuable insights into its effectiveness, limitations, and areas that need refinement. Expanding on the existing real-time hand gesture recognition application and exploring its deployment in these domains would be a logical next step.

Considering this paper's emphasis on computational efficiency in this paper, it would be highly relevant to investigate further advanced optimization methods to improve the framework's performance. Researching and implementing optimization techniques tailored to the framework's specific requirements can maximize its efficiency and effectiveness.

Lastly, conducting a comprehensive evaluation of the user experience (UX) would offer valuable feedback on the real-time application's usability and shape the direction of subsequent iterations and refinements. A dedicated UX study can provide insights from users into potential areas for refinement and enhancement. Exploring these future research avenues will advance dynamic hand gesture recognition and provide valuable insights into the practicality, performance optimization, and user-centric aspects of the developed framework.

REFERENCES

- [1] K. Lai and S. Yanushkevich, "An Ensemble of Knowledge Sharing Models for Dynamic Hand Gesture Recognition," *arXiv:2008.05732 [cs]*, Aug. 2020, arXiv: 2008.05732. [Online]. Available: <http://arxiv.org/abs/2008.05732>
- [2] C. Li, S. Li, Y. Gao, X. Zhang, and W. Li, "A Two-stream Neural Network for Pose-based Hand Gesture Recognition," *arXiv:2101.08926 [cs]*, Jan. 2021, arXiv: 2101.08926. [Online]. Available: <http://arxiv.org/abs/2101.08926>
- [3] J. Liu, Y. Liu, Y. Wang, V. Prinet, S. Xiang, and C. Pan, "Decoupled Representation Learning for Skeleton-Based Gesture Recognition," 2020, pp. 5751–5760. [Online]. Available: https://openaccess.thecvf.com/content_CVPR_2020/html/Liu_Decoupled_Representation_Learning_for_Skeleton-Based_Gesture_Recognition_CVPR_2020_paper.html
- [4] F. Yang, S. Sakti, Y. Wu, and S. Nakamura, "Make Skeleton-based Action Recognition Model Smaller, Faster and Better," *arXiv:1907.09658 [cs]*, Mar. 2020, arXiv: 1907.09658 version: 8. [Online]. Available: <http://arxiv.org/abs/1907.09658>
- [5] H. Gammulle, S. Denman, S. Sridharan, and C. Fookes, "TMMF: Temporal Multi-Modal Fusion for Single-Stage Continuous Gesture Recognition," *IEEE Transactions on Image Processing*, vol. 30, pp. 7689–7701, 2021, conference Name: IEEE Transactions on Image Processing.
- [6] G. Benitez-Garcia, J. Olivares-Mercado, G. Sanchez-Perez, and K. Yanai, "IPN Hand: A Video Dataset and Benchmark for Real-Time Continuous Hand Gesture Recognition," *arXiv:2005.02134 [cs]*, Oct. 2020, arXiv: 2005.02134. [Online]. Available: <http://arxiv.org/abs/2005.02134>
- [7] Z. Wang, Q. She, T. Chalasani, and A. Smolic, "CatNet: Class Incremental 3D ConvNets for Lifelong Egocentric Gesture Recognition," *arXiv:2004.09215 [cs, eess]*, Apr. 2020, arXiv: 2004.09215. [Online]. Available: <http://arxiv.org/abs/2004.09215>
- [8] C. Zhang, Y. Zou, G. Chen, and L. Gan, "PAN: Towards Fast Action Recognition via Learning Persistence of Appearance," *arXiv:2008.03462 [cs]*, Aug. 2020, arXiv: 2008.03462. [Online]. Available: <http://arxiv.org/abs/2008.03462>
- [9] Y. Min, Y. Zhang, X. Chai, and X. Chen, "An Efficient PointLSTM for Point Clouds Based Gesture Recognition," 2020, pp. 5761–5770. [Online]. Available: https://openaccess.thecvf.com/content_CVPR_2020/html/Min_An_Efficient_PointLSTM_for_Point_Clouds_Based_Gesture_Recognition_CVPR_2020_paper.html
- [10] A. Mohammed, Y. Gao, Z. Ji, J. Lv, S. Islam, and Y. Sang, "Automatic 3D Skeleton-based Dynamic Hand Gesture Recognition Using Multi-Layer Convolutional LSTM," in *Proceedings of the 7th International Conference on Robotics and Artificial Intelligence*, ser. ICRAI '21. New York, NY, USA: Association for Computing Machinery, Apr. 2022, pp. 8–14. [Online]. Available: <https://dl.acm.org/doi/10.1145/3505688.3505690>
- [11] J. Liu, Y. Wang, S. Xiang, and C. Pan, "HAN: An Efficient Hierarchical Self-Attention Network for Skeleton-Based Gesture Recognition," *arXiv:2106.13391 [cs]*, Jun. 2021, arXiv: 2106.13391. [Online]. Available: <http://arxiv.org/abs/2106.13391>
- [12] L. Shi, Y. Zhang, J. Cheng, and H. Lu, "Decoupled Spatial-Temporal Attention Network for Skeleton-Based Action Recognition," *arXiv:2007.03263 [cs]*, Jul. 2020, arXiv: 2007.03263. [Online]. Available: <http://arxiv.org/abs/2007.03263>
- [13] X. Yang, P. Molchanov, and J. Kautz, "Making Convolutional Networks Recurrent for Visual Sequence Learning," 2018, pp. 6469–6478. [Online]. Available: https://openaccess.thecvf.com/content_cvpr_2018/html/Yang_Making_Convolutional_Networks_CVPR_2018_paper.html
- [14] P. Molchanov, X. Yang, S. Gupta, K. Kim, S. Tyree, and J. Kautz, "Online Detection and Classification of Dynamic Hand Gestures with Recurrent 3D Convolutional Neural Networks," in *2016 IEEE Conference on Computer Vision and Pattern Recognition (CVPR)*. Las Vegas, NV, USA: IEEE, Jun. 2016, pp. 4207–4215. [Online]. Available: <http://ieeexplore.ieee.org/document/7780825/>
- [15] Z. Yu, B. Zhou, J. Wan, P. Wang, H. Chen, X. Liu, S. Z. Li, and G. Zhao, "Searching Multi-Rate and Multi-Modal Temporal Enhanced Networks for Gesture Recognition," *IEEE Transactions on Image Processing*, vol. 30, pp. 5626–5640, 2021, conference Name: IEEE Transactions on Image Processing.
- [16] K. Lupinetti, A. Ranieri, F. Giannini, and M. Monti, "3D dynamic hand gestures recognition using the Leap Motion sensor and convolutional neural networks," *arXiv:2003.01450 [cs, eess]*, Sep. 2020, arXiv: 2003.01450. [Online]. Available: <http://arxiv.org/abs/2003.01450>
- [17] Q. De Smedt, H. Wannous, J.-P. Vandeborre, J. Guerry, B. Le Saux, and D. Filliat, "SHREC'17 Track: 3D Hand Gesture Recognition Using a Depth and Skeletal Dataset," in *3DOR - 10th Eurographics Workshop on 3D Object Retrieval*, I. Pratikakis, F. Dupont, and M. Ovsjanikov, Eds., Lyon, France, Apr. 2017, pp. 1–6. [Online]. Available: <https://hal.archives-ouvertes.fr/hal-01563505>
- [18] Q. De Smedt, H. Wannous, and J.-P. Vandeborre, "Skeleton-Based Dynamic Hand Gesture Recognition," in *2016 IEEE Conference on Computer Vision and Pattern Recognition Workshops (CVPRW)*. Las Vegas, NV, USA: IEEE, Jun. 2016, pp. 1206–1214. [Online]. Available: <http://ieeexplore.ieee.org/document/7789643/>
- [19] G. Garcia-Hernando, S. Yuan, S. Baek, and T.-K. Kim, "First-Person Hand Action Benchmark with RGB-D Videos and 3D Hand Pose Annotations," *arXiv:1704.02463 [cs]*, Apr. 2018, arXiv: 1704.02463. [Online]. Available: <http://arxiv.org/abs/1704.02463>

- [20] S. Y. Boulahia, E. Anquetil, F. Multon, and R. Kulpa, "Dynamic hand gesture recognition based on 3D pattern assembled trajectories," in *2017 Seventh International Conference on Image Processing Theory, Tools and Applications (IPTA)*, Nov. 2017, pp. 1–6, iSSN: 2154-512X.
- [21] K. Yun, J. Honorio, D. Chattopadhyay, T. L. Berg, and D. Samaras, "Two-person Interaction Detection Using Body-Pose Features and Multiple Instance Learning," in *2012 IEEE Computer Society Conference on Computer Vision and Pattern Recognition Workshops*, Jun. 2012, pp. 28–35, iSSN: 2160-7516.
- [22] A. Sabater, I. Alonso, L. Montesano, and A. C. Murillo, "Domain and View-point Agnostic Hand Action Recognition," *arXiv:2103.02303 [cs]*, Oct. 2021, arXiv: 2103.02303. [Online]. Available: <http://arxiv.org/abs/2103.02303>
- [23] Z. Deng, Q. Gao, Z. Ju, and X. Yu, "Skeleton-Based Multifeatures and Multistream Network for Real-Time Action Recognition," *IEEE Sensors Journal*, vol. 23, no. 7, pp. 7397–7409, Apr. 2023, conference Name: IEEE Sensors Journal.
- [24] A. S. M. Miah, M. A. M. Hasan, and J. Shin, "Dynamic Hand Gesture Recognition Using Multi-Branch Attention Based Graph and General Deep Learning Model," *IEEE Access*, vol. 11, pp. 4703–4716, 2023, conference Name: IEEE Access.
- [25] J.-H. Song, K. Kong, and S.-J. Kang, "Dynamic Hand Gesture Recognition Using Improved Spatio-Temporal Graph Convolutional Network," *IEEE Transactions on Circuits and Systems for Video Technology*, vol. 32, no. 9, pp. 6227–6239, Sep. 2022, conference Name: IEEE Transactions on Circuits and Systems for Video Technology.
- [26] M. R. Morris, "AI and Accessibility," *Communications of the ACM*, vol. 63, no. 6, pp. 35–37, May 2020. [Online]. Available: <https://dl.acm.org/doi/10.1145/3356727>
- [27] W. Mucha and M. Kämpel, "Beyond Privacy of Depth Sensors in Active and Assisted Living Devices," in *The 15th International Conference on Pervasive Technologies Related to Assistive Environments*. Corfu Greece: ACM, Jun. 2022, pp. 425–429. [Online]. Available: <https://dl.acm.org/doi/10.1145/3529190.3534764>
- [28] O. Köpüklü, N. Köse, and G. Rigoll, "Motion Fused Frames: Data Level Fusion Strategy for Hand Gesture Recognition," *arXiv:1804.07187 [cs]*, Apr. 2018, arXiv: 1804.07187. [Online]. Available: <http://arxiv.org/abs/1804.07187>
- [29] C. C. d. Santos, J. L. A. Samatelo, and R. F. Vassallo, "Dynamic Gesture Recognition by Using CNNs and Star RGB: a Temporal Information Condensation," *arXiv:1904.08505 [cs]*, Sep. 2019, arXiv: 1904.08505. [Online]. Available: <http://arxiv.org/abs/1904.08505>
- [30] M. Abavisani, H. R. V. Joze, and V. M. Patel, "Improving the Performance of Unimodal Dynamic Hand-Gesture Recognition With Multimodal Training," 2019, pp. 1165–1174. [Online]. Available: https://openaccess.thecvf.com/content_CVPR_2019/html/Abavisani_Improving_the_Performance_of_Unimodal_Dynamic_Hand-Gesture_Recognition_With_Multimodal_CVPR_2019_paper.html
- [31] G. Devineau, W. Xi, F. Moutarde, and J. Yang, "Deep Learning for Hand Gesture Recognition on Skeletal Data," May 2018. [Online]. Available: <https://hal-mines-paristech.archives-ouvertes.fr/hal-01737771>
- [32] M. Rehan, H. Wannous, J. Alkheir, and K. Aboukassam, "Learning Co-occurrence Features Across Spatial and Temporal Domains for Hand Gesture Recognition," in *Proceedings of the 19th International Conference on Content-based Multimedia Indexing*, ser. CBMI '22. New York, NY, USA: Association for Computing Machinery, Oct. 2022, pp. 36–42. [Online]. Available: <https://dl.acm.org/doi/10.1145/3549555.3549591>
- [33] O. Yusuf and M. Habib, "Development of a Lightweight Real-Time Application for Dynamic Hand Gesture Recognition," in *2023 IEEE International Conference on Mechatronics and Automation (ICMA)*, Aug. 2023, pp. 543–548, iSSN: 2152-744X.
- [34] A. Kendall, Y. Gal, and R. Cipolla, "Multi-Task Learning Using Uncertainty to Weigh Losses for Scene Geometry and Semantics," Apr. 2018, arXiv:1705.07115 [cs]. [Online]. Available: <http://arxiv.org/abs/1705.07115>
- [35] H. Sahbi, "Skeleton-based Hand-Gesture Recognition with Lightweight Graph Convolutional Networks," *arXiv:2104.04255 [cs]*, Apr. 2021, arXiv: 2104.04255. [Online]. Available: <http://arxiv.org/abs/2104.04255>
- [36] X. S. Nguyen, L. Brun, O. Lézoray, and S. Bougleux, "A neural network based on SPD manifold learning for skeleton-based hand gesture recognition," *arXiv:1904.12970 [cs]*, Apr. 2019, arXiv: 1904.12970. [Online]. Available: <http://arxiv.org/abs/1904.12970>
- [37] Y. Chen, L. Zhao, X. Peng, J. Yuan, and D. N. Metaxas, "Construct Dynamic Graphs for Hand Gesture Recognition via Spatial-Temporal Attention," *arXiv:1907.08871 [cs]*, Jul. 2019, arXiv: 1907.08871. [Online]. Available: <http://arxiv.org/abs/1907.08871>
- [38] K. Lai and S. N. Yanushkevich, "CNN+RNN Depth and Skeleton based Dynamic Hand Gesture Recognition," in *2018 24th International Conference on Pattern Recognition (ICPR)*, Aug. 2018, pp. 3451–3456, arXiv:2007.11983 [cs]. [Online]. Available: <http://arxiv.org/abs/2007.11983>
- [39] X. Chen, H. Guo, G. Wang, and L. Zhang, "Motion Feature Augmented Recurrent Neural Network for Skeleton-based Dynamic Hand Gesture Recognition," *2017 IEEE International Conference on Image Processing (ICIP)*, pp. 2881–2885, Sep. 2017, arXiv: 1708.03278. [Online]. Available: <http://arxiv.org/abs/1708.03278>
- [40] J. Weng, M. Liu, X. Jiang, and J. Yuan, "Deformable Pose Traversal Convolution for 3D Action and Gesture Recognition," 2018, pp. 136–152. [Online]. Available: https://openaccess.thecvf.com/content_ECCV_2018/html/Junwu_Weng_Deformable_Pose_Traversal_ECCV_2018_paper.html
- [41] X. Nguyen, L. Brun, O. Lézoray, and S. Bougleux, "Skeleton-Based Hand Gesture Recognition by Learning SPD Matrices with Neural Networks," May 2019, arXiv:1905.07917 [cs]. [Online]. Available: <http://arxiv.org/abs/1905.07917>
- [42] J. Chen, C. Zhao, Q. Wang, and H. Meng, "HMANet: Hyperbolic Manifold Aware Network for Skeleton-Based Action Recognition," *IEEE Transactions on Cognitive and Developmental Systems*, vol. 15, no. 2, pp. 602–614, Jun. 2023, conference Name: IEEE Transactions on Cognitive and Developmental Systems.
- [43] S. Song, C. Lan, J. Xing, W. Zeng, and J. Liu, "Spatio-Temporal Attention-Based LSTM Networks for 3D Action Recognition and Detection," *IEEE Transactions on Image Processing*, vol. 27, no. 7, pp. 3459–3471, Jul. 2018, conference Name: IEEE Transactions on Image Processing.
- [44] X. Liu, H. Shi, X. Hong, H. Chen, D. Tao, and G. Zhao, "3D Skeletal Gesture Recognition via Hidden States Exploration," *IEEE Transactions on Image Processing*, vol. 29, pp. 4583–4597, 2020, conference Name: IEEE Transactions on Image Processing.
- [45] A. Kacem, M. Daoudi, B. B. Amor, S. Berretti, and J. C. Alvarez-Paiva, "A Novel Geometric Framework on Gram Matrix Trajectories for Human Behavior Understanding," *IEEE Transactions on Pattern Analysis and Machine Intelligence*, vol. 42, no. 1, pp. 1–14, Jan. 2020, conference Name: IEEE Transactions on Pattern Analysis and Machine Intelligence.
- [46] Q. Ke, M. Bennamoun, S. An, F. Sohel, and F. Boussaid, "Learning Clip Representations for Skeleton-Based 3D Action Recognition," *IEEE Transactions on Image Processing*, vol. 27, no. 6, pp. 2842–2855, Jun. 2018, conference Name: IEEE Transactions on Image Processing.
- [47] J. Liu, G. Wang, L.-Y. Duan, K. Abdiyeva, and A. C. Kot, "Skeleton-Based Human Action Recognition With Global Context-Aware Attention LSTM Networks," *IEEE Transactions on Image Processing*, vol. 27, no. 4, pp. 1586–1599, Apr. 2018, conference Name: IEEE Transactions on Image Processing.
- [48] M. Maghoumi and J. J. LaViola Jr, "DeepGRU: Deep Gesture Recognition Utility," *arXiv:1810.12514 [cs]*, Oct. 2019, arXiv: 1810.12514. [Online]. Available: <http://arxiv.org/abs/1810.12514>
- [49] P. Zhang, C. Lan, J. Xing, W. Zeng, J. Xue, and N. Zheng, "View Adaptive Neural Networks for High Performance Skeleton-Based Human Action Recognition," *IEEE Transactions on Pattern Analysis and Machine Intelligence*, vol. 41, no. 8, pp. 1963–1978, Aug. 2019, conference Name: IEEE Transactions on Pattern Analysis and Machine Intelligence.